Serial No. 558,998

Filing Date 16 November 1995

Inventor David H.C. Stoudt
Michael A. Richardson

NOTICE

The above identified patent application is available for licensing. Requests for information should be addressed to:

OFFICE OF NAVAL RESEARCH
DEPARTMENT OF THE NAVY
CODE OOCC3
ARLINGTON VA 22217-5660

DISTRIBUTION STATEMENT A
Approved for public release;
Distribution Unlimited

19960409 199

DISCLAIMER NOTICE

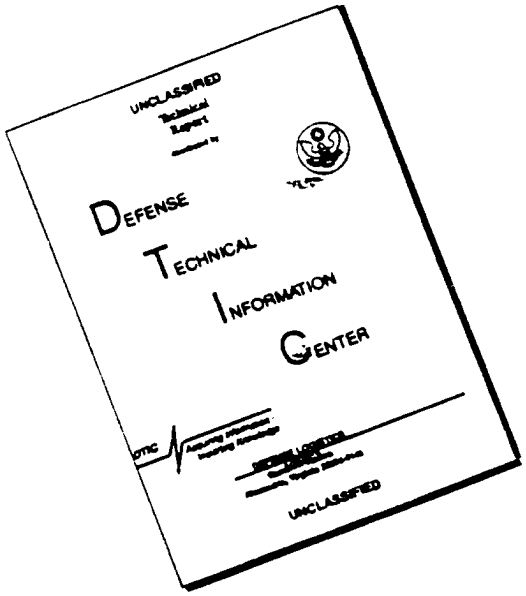

THIS DOCUMENT IS BEST QUALITY AVAILABLE. THE COPY FURNISHED TO DTIC CONTAINED A SIGNIFICANT NUMBER OF PAGES WHICH DO NOT REPRODUCE LEGIBLY.

Navy Case: 76,968
1-703-663-8061
Dahlgren, VA 22448

BISTABLE PHOTOCONDUCTIVE SWITCHES PARTICULARLY SUITED FOR FREQUENCY-AGILE, RADIO-FREQUENCY SOURCES

STATEMENT OF GOVERNMENT INTEREST

The invention described herein was made by employees of the United States Government and may be manufactured and used by or for the Government for governmental purposes without the payment of any royalties thereon or therefor.

FIELD OF THE INVENTION

This invention relates generally to semiconductors and radio frequency (RF) sources, and relates specifically to both a fabrication process for making copper-compensated, silicon-doped, gallium arsenide (GaAs) bistable, photoconductive switches and circuit arrangements thereof. These switches are particularly suited to provide high-speed, high-power, frequency-agile RF sources.

BACKGROUND OF THE INVENTION

In recent years there has been considerable interest in the development of high-speed, high-power photoconductive switches for use in direct dc, or quasi-dc, to RF conversion thereof. The applications for this type of technology are primarily in the area of ultra-wide-band (UWB) radar, impulse radar, biological-effects testing, and high-speed diagnostic equipment. These applications require that the switching speeds be as fast as possible so that the generated electrical pulses contain the highest possible frequency components.

A recently introduced photoconductive switch, which is called the bistable (or bulk) optically controlled semiconductor switch (BOSS), (herein termed a BOSS switch) is disclosed in U.S. Patent No. 4,825,061 ('061) of Schoenbach, et al, herein incorporated by reference. The operation of the BOSS switch disclosed in the '061 patent relies on persistent photoconductivity, which can be considered a gain mode, followed by photo-induced quenching to provide both BOSS switch closing and opening, respectively. A semi-insulating GaAs material is used in this BOSS switch and is manufactured by controlled electrical compensation of silicon-doped GaAs with copper (GaAs:Si:Cu). The process by which the GaAs:Si:Cu material may be manufactured is disclosed in U.S. Patent No. 5,374,589 ('589) of Roush, et al teaching a thermally diffused copper process, herein incorporated by reference. We have

determined that the BOSS switches formed of this copper-compensated, silicon-doped material (GaAs:Si:Cu) described in the '061 patent and manufactured by the thermal diffusing process of the '589 patent suffer a drawback in their inability to switch to their open or high resistance state in response to a subnanosecond light pulse having an operating wavelength in the 2-micron regime. This drawback limits the radio-frequency range for the applications of BOSS switches.

It is therefore an important object of the present invention to provide BOSS switches that may be switched into their open, high resistance state in response to a subnanosecond light pulse.

SUMMARY OF THE INVENTION

The invention is directed to a method of enhancing the speed of response of a photoconductive switch, such as a BOSS switch so that ~~it~~ may be switched into its open or high resistance state in response to a subnanosecond light pulse. The invention is also directed to circuit arrangements provided by these improved BOSS switches.

The photoconductive switch has a predetermined recombination center density created by neutron irradiation and also has closed low-resistance and open high resistance states, wherein the open

state is achieved within a time less than 1 nanosecond in response to a light pulse. The photoconductive switch is preferably comprised of GaAs:Si:Cu, wherein Cu forms a deep acceptor level Cu_B in said GaAs at an energy level of about 0.44eV above a valence band.

Accordingly, it is a primary object of the present invention to provide a photoconductive switch that is responsive to a light pulse in the subnanosecond regime so as to switch the device into its open state possessing a high electrical resistance.

It is a further object of the present invention to subject photoconductive switching device to neutron irradiation so as to increase the density of its recombination centers to enhance the speed of its response, especially the speed of response of the photoconductive switching device to a light signal in the subnanosecond regime so as to switch the photoconductive device into its high electrical resistant state.

It is a further object of the present invention to arrange one or more photoconductive switching devices, each having an improved speed of response, into a generator particularly suited for RF application and which may be configured onto a microstrip arrangement.

Further still, it is an object of the present invention to

provide for a pulse-switch-out (PSO) generator capable of switching relatively high positive and negative voltage potentials.

Other objects, advantages and novel features of the invention will become apparent from the following detailed description when considered in conjunction the accompanying drawings herein.

BRIEF DESCRIPTION OF THE DRAWINGS

Fig. 1 is an energy-level diagram showing the dominant impurity levels of a semiconductor material preferably used for the photoconductive switch of the present invention.

Fig. 2 is composed of Figs. 2(A), (B), (C), (D), (E), and (F) and illustrate the overall operation of the photoconductive switch of the present invention.

Fig. 3 is a schematic diagram of a pulse-switch-out (PSO) generator that utilizes two photoconductive switches of the present invention.

Fig. 4 illustrates a stripline configuration of the PSO generator of Fig. 3.

Fig. 5 is a schematic diagram of an experimental setup used in

the practice of the present invention.

Fig. 6 illustrates the pulse-width agility achieved by varying the time delay between laser pulses directed onto the photoconductive switch of the present invention.

Fig. 7 illustrates various repetition rates, within a two-pulse burst, at an applied relatively high voltage in the range of about 16kV.

Fig. 8 illustrates a Fourier spectra of the waveforms of Fig. 7.

Fig. 9 primarily illustrates an optical delay line used in the evaluation of the photoconductive switches of the present invention.

Fig. 10 illustrates two bipolar pulses produced by a PSO generator of Figs. 3 and 4.

Fig. 11 illustrates the Fourier spectra of the two bipolar pulses of Fig. 10.

Fig. 12 illustrates replicating data similar to that shown in Fig. 10.

Fig. 13 illustrates a power spectrum of a single monocycle waveform having a repetition rate of 1kHz.

Fig. 14 illustrates a power spectrum of the waveforms of Fig. 12 having a 1kHz burst-repetition rate.

Fig. 15 illustrates replicating data of the bipolar pulses shown in Fig. 10.

Fig. 16 illustrates a power spectrum of the waveforms of Fig. 15 having a 1kHz burst-repetition rate.

DETAILED DESCRIPTION OF THE PREFERRED EMBODIMENTS

In general, the present invention relates to a photoconductive switching device, such as a semiconductor switch commonly referred to as a BOSS switch disclosed in both the previously mentioned U.S. Pat~~ents~~ 4,825,061 ('061) and 5,374,589 ('589). However, unlike the BOSS switch disclosed in the '061 and '589 patents, the photoconductive switch of the present invention obtains its closed, low-resistance and open, high electrical resistance state, each within a time less than 1 nanosecond, in response to the application of a light pulse, such as a laser beam. The achievement of this less than 1 nanosecond response is achieved by neutron-irradiation of BOSS switches which increases the density of

recombination centers in the material GaAs:Si:Cu, preferably used for the photoconductive switch of the present invention. The various energy levels of interest within the bandgap of GaAs:Si:Cu at 25°C is shown in Fig. 1 and has the parameters given in Table 1:

TABLE 1

REFERENCE NUMBER/LETTER	GENERAL DEFINITION
12 (Ec)	Conduction Band
14 (E_{si})	Silicon Shallow Donor having a typical value of 5.8meV below conduction band 12
16 (E_F)	Fermi Level
18 (E_{CuB})	Electron Level of Cu_B Deep Acceptor having a typical value of 0.44eV above valence band 20
20 (E_V)	Valence Band
Cu_B	Copper Dominant Deep Acceptor Level
Cu_A	Copper Dominant Deep Acceptor Level having a typical value of 0.14eV above valence band 20
EL2	Deep Donor Level Native to GaAs and having a typical value of 0.83eV below conduction band 12
RC	Recombination Center having an approximate value of 0.67eV below conduction band 12
Bandgap	Bandgap having a typical value of 1.42eV as measured between the conduction band 12 and valence band 20 and commonly referred to as hv

The location of the recombination center RC, to be further described hereinafter, shown in Fig. 1 is an approximate, not precise, value. The copper, Cu, used in the material GaAs:Si:Cu forms two dominant deep acceptor levels in GaAs, at 0.14eV (Cu_A) and 0.44eV (Cu_B) both above the valence band 20. The Cu_B level is the copper level of primary interest of the photoconductive switching device of the present invention and is interchangeably referred to herein as "Cu_B center."

The photo-ionization cross section of holes ($10^{-16}cm^2$) and of electrons ($10^{-17}cm^2$) for the Cu_B level in GaAs, which are of importance to the present invention, were measured by Kullendorf, et al, as described in the technical article "Copper-Related Deep Level Defects in III-V Semiconductors," published in J.Appl. Phys., Vol. 54, pp. 3203-3212, 1983 and herein incorporated by reference. In addition, the capture cross sections for holes and electrons in the Cu_B center, also important to the present invention, are $3x10^{-14}cm^2$ and $8x10^{-21}cm^2$, respectively, as described by D. V. Lang and ~~R.A.~~ Logan, in the technical article "A Study of Deep Levels in GaAs by Capacitance Spectroscopy," published in the J. Electronic Materials, Vol. 4, pp. 1053-1066, 1975, and also herein incorporated by reference. The large ratio of the hole to electron capture cross sections make the Cu_B center a very strong hole trap. When the proper amount of copper is diffused into the GaAs:Si material to result in a semi-insulating behavior, as is the case in the present invention, the electron Fermi level 16 of Fig. 1 is

above the Cu_B level. Therefore, the Cu_B center is mostly full of electrons under the conditions of thermodynamic equilibrium. This fact, as well as the large ratio of capture cross sections for holes and electrons in the Cu_B center, is of importance to the present invention. The operation of the present invention may be further described with reference to Fig. 2 composed of Figs. 2(A), (B), (C), (D), (E) and (F).

One possible photoconductive switch geometry, shown in Fig. 2(A), is sometimes referred to as a lateral switch and is generally indicated with the reference number 22. The photoconductive switch 22 comprises a bulk piece 24 of semi-insulating material, sometimes referred to as substrate, with two electrical contacts 26 and 28 operatively connected to the substrate 24, in a manner known in the art, and herein termed "electrical-contact gaps." The electrical-contact gaps 26 and 28 are preferably located at opposite ends of the substrate 24 and each has a length in the range from about less than about 1 micrometer to greater than about 1 centimeter. It is further preferred that the electrical-contact gaps 26 and 28 be located at opposite ends of the same surface of the substrate 24. The electrical-contact gaps 26 and 28 are operatively connected to electrically conductive elements 30 and 32, respectively, wherein conductive element 30 may be arranged to serve as an input port and receive an input signal (not shown) and conductive element 32 may be arranged to serve as an output port and provide an output signal from the photoconductive switch 22.

The photoconductive switch 22 has a third port 34 located between the electrical-contact gaps 26 and 28 and arranged to receive optical illumination. The photoconductive switch 22 may serve as a BOSS switch described in the previously incorporated by reference patents '061 and '589. The optical illumination impinging on the BOSS switch 22 may comprise first and second light beams 36 and 38 respectively having first and second wavelengths, with the second wavelength being longer than the first wavelength. The first and second wavelengths may respectively have typical values of about 1 and 2 micrometers, respectively. The first and second light beams are preferably laser beams supplied from a Nd:YAG laser, fitted with an optical parametric generator (OPG). The laser beams 36 and 38 may be interchangeably referred to herein as turn-on, turn-off lasers.

Figs. 2(B), (C), (D), (E), and (F), respectively illustrate (a) the resulting current delivered to a load during the switching cycle of the BOSS switch 22, (b) the initial high-resistive state of material (GaAs:Si:Cu) prior to the first laser beam 36, (c) the optical excitation of electrons from the Cu_B center to the conduction band 12, (d) the slow decay of electrons during the on state of the BOSS switch 22, and (e) the fast photo-induced quenching of the photoconductivity of the BOSS switch 22.

As seen in Fig. 2(B), the current that is permitted to flow through external circuit (not shown) has a waveform 40 comprising

an on-state (42) and an off-state (44). The on-state 42 has a period determined by the difference between times t_1 and t_2, whereas the off-state 44 is determined by the selected duty cycle of the BOSS switch 22.

As seen in Fig. 2(C), for ideal switching conditions for the BOSS switch 22 all thermally ionized electrons 46 from the silicon level 14(E_{si}) are trapped in the Cu_B center illustrated as being at electron level 16 (E_{CuB}). Further, as seen in Fig. 2(C) holes 48 are located between the silicon level 14 and the conduction band 12. The ideal conditions of Fig. 2(C) represent that the trapping of the electrons in the Cu_B center results in an electrically compensated, high-resistivity material, and the state of the BOSS switch 22 when voltage (to be described) is first applied. In this condition, the BOSS switch 22 may be illuminated with the laser beam 36 that supplies photon energy sufficient, as illustrated in Fig. 2(D), to elevate, as indicated by directional arrow 50, the electrons 46 from the Cu_B center to the conduction band 12. The supply of photon energy is realized by the laser beam 36 having a typical fundamental wavelength of a Nd:YAG laser, λ=1.06 micrometer.

As further seen in Fig. 2(D), at the same time electrons 46 are elevated from the Cu_B center, holes 48 are generated in the valence band 20 through photonionization of empty Cu_B levels. As the laser pulse 36 is terminated, there is a period of fast

electron-hole recombination, as indicated by directional arrow 52, through the recombination center (not depicted in Fig. 2.). However, due to the large cross-section of Cu_B for hole trapping, a sufficient density of holes are re-trapped to allow a large free-electron density to remain in the conduction band. Therefore, current is permitted to flow through the external circuit as previously discussed with reference to Fig. 2(B) and as shown by on-state 42 thereof. Because the electron capture cross-section of Cu_B is much smaller than the hole capture cross-section of Cu_B, the electrons in the conduction band 12 will remain for relatively long periods of time, as generally illustrated in Fig. 2(E) by phantom directional arrow 54, after the first laser beam 36 is terminated. The long lifetime of electrons in the conduction band 12 makes GaAs:Si:Cu a high-gain photoconductor material because current will flow to an external circuit for a relatively long time after the turn-on laser beam 36 is terminated.

The current through the BOSS switch 22 can now be terminated by illuminating the GaAs crystal with photons of energy that is less than the Cu_B-to-conduction-band transition (approximately 1.42eV-0.44eV = 0.98eV), but greater than the valence-band-to-Cu_B transition (0.44eV < hv < 0.98eV). The second laser beam 38 may supply this illumination and may have a typical wavelength of a wavelength-doubled Nd:YAG laser, λ = 2.13 micrometers. These photons will elevate, as indicated by directional arrow 56, electrons 46 back into the Cu_B level, leaving behind holes 48 in

the valence band 20 which can then recombine, as indicated by directional arrow 58 with the free electrons in the conduction band 16, thus leading to the opening of the BOSS switch 22 (see Fig. 2(F)) on a nanosecond time scale. In a desired case, the second laser beam 38 would reset the GaAs:Si:Cu material 24 back to its initial condition (see Fig. 2(C)) prior to the first laser beam 36. The BOSS switch 22 may be operated at high-repetition rates and also to switch relatively high power levels.

METHOD OF FORMING THE PHOTOCONDUCTIVE SWITCH OF THE PRESENT INVENTION

As discussed in the "Background" section, we have determined that the GaAs:Si:Cu material produced by a thermal diffusion process, without the benefits of the present invention, contains an insufficient number of recombination centers to allow a photoconductive switch, such as a BOSS switch, to open in the subnanosecond regime. Therefore, in accordance with the practice of the present invention we provide the means to create a higher density of recombination centers in the GaAs crystal to allow for BOSS switch 22 to open in the subnanosecond regime. Fast-neutron irradiation is selected to introduce this higher density of recombination centers, each possessing a near-mid-bandgap energy level such as 0.67eV illustrated in Fig. 1. It is preferred that the density of recombination centers be within the range from about $5x10^{15}cm^{-3}$ to about $5x10^{16}cm^{-3}$.

The effects of neutron irradiation on semiconducting materials have been studied for many years. A recent effort has concentrated on the reduction of the minority-carrier lifetime in GaAs through fast-neutron irradiation as disclosed by C. L. Wang, et al, in the technical article "Neutron-Treated, Ultrafast, Photoconductor Detectors," published in Appl. Phys. Lett., Vol. 54, pp. 1451-1453, 1989, and herein incorporated by reference. This work by Wang et al indicated that the crystal damage created by neutron irradiation could be used for the purpose of recombination center enhancement in a BOSS switch that is based on a GaAs:Si:Cu material. However, unlike the present invention, the work of Wang et al is silent on any teaching of any intensity neutron irradiation, within any desired range, needed to improve the response time of the BOSS switch.

The unit for describing the intensity of neutron radiation is flux in units of neutrons/cm^2-s. The time integral of the flux, called the fluence, has the units of neutrons/cm^2 and is designated by ~~the~~ symbol Φ. Fluence is the common term used in radiation effects field to describe neutron exposure. Another important characteristic of radiation is the energy spectrum. The neutron source used in our work was Sandia National Laboratory's SPR-III bare core reactor. Special precautions were taken in our work to insure that the sample temperature, that is the temperature of the BOSS switch 22 of our invention receiving neutron irradiation, did not rise about 100°C during the time that the samples were being

exposed. The energy spectrum of this source used to provide neutron irradiation of our samples, is peaked at about 1MeV. A boron shield was used during the irradiations or our photoconductive switch to absorb thermal neutrons below 10keV. Accordingly, it is preferred that the energy spectrum for neutron irradiation, used in the practice of our invention, range from 10keV to 1MeV.

Our BOSS switch 22 was irradiated with energetic neutrons following the thermal diffusion of copper into the GaAs material, more fully described in the '589 patent, and both before and after the electrical-contact gaps 26 and 28 (see Fig. 2(A)) were fabricated onto the GaAs substrate 24. Thus far, many BOSS switches have been irradiated at multiple fluence levels and have been experimentally tested to determine the results of the irradiation. The neutron irradiation enhances the speed of response of the BOSS switches 22 as shown from our experimental testing to be more fully described hereinafter. Two samples (Sample A and Sample B) were experimentally tested in which Sample A received neutron irradiation at a relatively low fluence measured at $2.45 \times 10^{15} cm^{-2}$, whereas Sample B received neutron irradiation at a relatively high fluence measured at $3.93 \times 10^{15} cm^{-2}$. The dc I-V characteristics of the samples A and B indicated an increase in the switch resistance (open-state, see Fig. 2(F)) from about 3.2MΩ (measured prior to neutron irradiation) to about 55MΩ for the lower fluence irradiation, and an increase from about 4.3MΩ (measured

prior to neutron irradiation) to about 273MΩ for the higher fluence irradiation.

SWITCHING APPLICATIONS OF THE PHOTOCONDUCTIVE SWITCH OF THE PRESENT INVENTION

The ability of a BOSS switch, not having the benefits of the present invention, preferably made from GaAs:Si:Cu, to close and open has been demonstrated at relatively high power levels on the several-nanosecond time scale by D.C. Stoudt, et al, as disclosed in the technical article "Characterization and Switching Study of an Optically Controlled GaAs switch," published Proc. SPIE, Vol. 1378, Optically Activated Switching, 1990, pp. 280-285; and again by D.C. Stoudt, et al, as described in the technical article, "Investigation of a Laser-Controlled, Copper-Doped GaAs Closing (low resistance state) and Opening (high resistance state) Switch for Pulsed Power Applications," published Proc. 8th IEEE Pulsed Power Conf., San Diego, CA. 1991, pp. 41-45, both of such technical articles being herein incorporated by reference. Recent experimental results have shown that the current through a BOSS switch could not be fully quenched (turned-off) by the application of a 140ps full width at half magnitude (FWHM) 2.13μm laser pulse as described by M.S. Mazzola et al, in the technical article "Subnanosecond Performance of the BOSS GaAs Opening Switch," published in Proc. 20th Power Mod. Symp., Myrtle Beach, SC, 1992, pp. 266-270 and which is herein incorporated by reference. A

numerical solution of the semiconductor rate equations for copper-doped GaAs showed that the primary cause for incomplete photo-quenching, on the subnanosecond time scale, such as described by M.S. Mazzola et al, was that the concentration of the recombination centers was too low. This numerical solution was disclosed by D.C. Stoudt, et al, in the technical article "Effects of 1MeV Neutron Irradiation on the Operation of a Bistable Optically Controlled Semiconductor Switch (BOSS)," published in IEEE Trans. Electron Dev., Vol. 41, pp. 913-919, 1994. Again, like the previously mentioned work of Wang et al, the extensive works of M.S. Mazzola et al and D.C. Stoudt et al are silent on any teaching related to the present invention of any neutron irradiation within any desired range needed to improve the response time of the BOSS switch to the subnanosecond regime.

The transition for placing the BOSS switch 22 conducting relatively high power levels into its high electrical resistance state is the result of a two-step process, with one step being controlled by the electron-hole recombination lifetime which is dominated by the concentration of mid-gap recombination centers in the bulk material. For example, the recombination centers located in the mid-region of the bandgap (hv) such as the recombination center RC of Fig. 1 having an energy level of approximately 0.67eV and approximately located in the mid-region of the bandgap (hv) of Fig. 1.

A recombination center (RC) is considered to occur when the cross-sections for electron and hole capture are approximately equal. If there is an insufficient recombination center concentration, the holes that are generated by the light pulse, such as 2μm laser pulse (second laser beam 38 of Fig. 2(A)) commonly applied to turn off the BOSS switch, are re-trapped in the copper centers, such as Cu_B, before the holes have an opportunity to recombine with electrons in the conduction band. This re-trapping disadvantageously results in the switch remaining closed after the termination of the second laser beam 38 of Fig. 2(F). The present invention eliminates this problem by neutron irradiation of the BOSS switch 22 to supply a sufficient number of recombination centers to prevent re-trapping of holes and allow BOSS switch 22 to sequence into its open (high resistant) state after the laser beam 38 is terminated.

One potential application for the BOSS technology having the benefits of the present invention is a wideband, frequency-agile source that can radiate the RF energy with a broadband antenna. For such an application, in order to maximize the radiative efficiency of the source, it is necessary to produce ac power which reduces the dc component of the waveform. This is important since the dc component cannot be radiated out of an antenna. The ability of the BOSS switch 22 of the present invention to open, as well as close, in the subnanosecond regime allows a unique type of RF source to be developed that is capable of generating repetitive

high-power microwave cycles of varying duration, depending on the relative delay between the turn-on and turn-off laser pulses, such as laser beams 36 and 38 respectively, of Fig. 2(A).

An RF source configuration that makes use of the benefits of the present invention and that is capable of generating ac power with real-time frequency agility (known in the art) is shown in Fig. 3 and is commonly called a pulse-switch-out (PSO) generator. The PSO generator 60 of Fig. 3 comprises a first BOSS switch 22A and a second BOSS switch 22B each having the energy levels, in particular, the recombination center RC illustrated in Fig. 1. The BOSS switches 22A and 22B have input connections 30A and 30B, respectively, and output connections 32A and 32B, respectively, previously described, in general, with reference to Fig. 2(A). The input connections 30A and 30B are respectively connected to one end of charged transmission lines 62 and 64 which have their other end respectively connected to a relatively high positive (+V) potential 66 and a relatively high negative (-V) potential 68. Both output connections 32A and 32B are preferably connected to one end of common transmission line 70 which has its other end connected to a load R_L that may represent a broadband antenna. The operation, to be described, of the PSO generator 60 generates an output voltage 72 having positive half-cycles 74 and negative half-cycles 76 as shown in Fig. 3. The time between pulses 74 represents the time between closures of BOSS switch 22A and is indicated by dimensional line 78 and the time between pulses 76 represents the time between

closures of BOSS switch 22B and is indicated by dimensional line 80. Positive (74) and negative (76) half-cycles, serves as RF pulses, are generated by first closing and then opening each BOSS switch 22A and 22B in succession. The frequency content in the generated RF pulses 74 and 76, as will be further described, can be adjusted by either varying the time between the closure of each BOSS switch 22A and 22B, or by varying the time between the closure of each BOSS switch 22A and 22B while keeping the electrical pulse width the same. The PSO generator 60 may be arranged in a variety of ways, one of which is shown on a microstrip line 82 in Fig. 4.

The basic advantages of the PSO generator 60 arranged on the microstrip 82 (known in the art) have been demonstrated and which comprises two 50Ω charged transmission lines 62 and 64 that feed through the two BOSS switches 22A and 22B (embedded in the microstrip 82) into a single common 50Ω transmission line 70 that ultimately leads to either a matched load R_L, or to an antenna (not shown) if it is desired to radiate the RF energy. Making the two BOSS switches 22A and 22B attached to the same point of the common transmission line 70 greatly reduces the severity of reflections, to be further described, seen by the PSO generator 60 serving as a source. Therefore, the fidelity of the waveforms 74 and 76 of RF output signal 72 is enhanced. It is important to realize that the ability of the BOSS switches 22A and 22B to each open, thus interrupting the current, while voltage is left on the charged transmission lines 62 and 64, respectively, means that the

impedance of the charged transmission line, such as 62 or 64, does not necessarily have to match the impedance of the common transmission line 70. Thus, if the impedance of the charged transmission line 62 or 64 was reduced to a value that was much less than the impedance of the common transmission line 70, then the voltage (+V(66) or -V(68)) delivered to the load R_L would be roughly equivalent to the total charge voltage carried by charged transmission lines 62 and 64, respectively, rather than half of the charge voltage, as in the matched transmission line cases. This arrangement results in a factor of four increase in the power delivered to the load R_L for a given charge voltage.

The PSO generator 60 of Figs. 3 and 4 could also be used as a means for generating ac power to be delivered to any load. A possible example would be for use in a switching power supply. The PSO generator 60 could also be used in many high-speed diagnostic applications where both high and low power, high-bandwidth pulses are required. The PSO generator 60 has further applications to be described hereinafter.

TEST EVALUATION OF THE PHOTOCONDUCTIVE SWITCH OF THE PRESENT INVENTION

In the practice of the present invention, BOSS-switching experiments were conducted with a mode-locked Nd:YAG laser system producing a first laser beam having an operating wavelength of 1.06μm and manufactured by Continuum Inc., that was equipped with

an optical parametric generator (OPG), known in the art, which served to double the wavelength so as to provide a second laser beam having an operating wavelength of 2.13μm. Thus, two laser beams were provided. The first having an operating wavelength of 1.06μm serving as laser beam 36 of Fig. 2(A) to turn-on (low resistance path) BOSS switch 22 and the second having an operating wavelength of 2.13μm serving as laser beam 38 of Fig. 2(A) to turn-off (high resistance path) BOSS switch 22. A laser system 84 was used as a setup to test the BOSS switch 22 as shown in Fig. 5 and comprises a ND:YAG laser source 86 and an OPG 88.

The laser system 84 produced a Gaussian pulse with a FWHM of about 140ps. A simple optical delay line (not shown in Fig. 5, but an optical delay line is to be described with reference to Fig. 10) was then used to adjust the time between the closure of BOSS switch 22 and the opening of BOSS switch 22. Photoconductivity measurements were performed to evaluate the operation of the neutron irradiated BOSS device 22 of the present invention. The BOSS switch 22 was embedded in a 50Ω transmission line 90 (two-way transit time ≈ 8ns) that was pulse charged with roughly a 40ns FWHM voltage pulse generated by a Klystron circuit 92 (known in the art) arranged as shown in Fig. 5. The maximum voltage applied to the BOSS switch 22 was about 18kV. The current through the BOSS switch 22 was measured by a 50Ω current-viewing resistor (CVR) (not shown), known in the art, placed after the BOSS switch 22 in the 50Ω line 70. The current waveform was recorded by a Tektronix

SCD5000 digitizer 94 having a 3.0GHz analog/digital bandwidth. The results were also recorded on a conventional computer workstation 96.

The experimental testing was performed on the two previously mentioned Samples A and B, with Sample A receiving a neutron irradiation of a fluence of 2.45×10^{15} cm^{-2} and Sample B receiving a neutron irradiation of a fluence of $3.93 \times 10^{15} cm^{-2}$. Switching results illustrating a photocurrent 98 for Sample A are shown in Fig. 6 for an applied voltage of 3.7kV. The maximum voltage that was switched with this BOSS switch 22 was about 18kV. This 18kV value was caused by the bias-voltage modulator limitation of the test equipment, and not by the limitation of the BOSS switch 22. It is contemplated that switching voltages in the range of 25kV to 50kV should be possible with the neutron-irradiated BOSS switches 22 of the present invention. During our testing, the switching behavior of Sample A did not change as the applied voltage was increased.

Fig. 6 shows several current waveforms 100_1 ... 100_N superimposed on waveform 98 to demonstrate the ability to control the pulse width of the electrical pulse delivered to the 50Ω CVR of Fig. 5. The laser pulse energy for both the 1.06μm and the 2.13μm wavelengths, serving as laser beams 36 and 38, was set at 4.5 millijoules (mJ). The minimum switch resistance during the transient from the off-on states was measured to be ≤1Ω. The minimum pulse width achieved with the BOSS switch 22 was measured

to be about 650ps FWHM. A curve fit to the switch conductance during the opening phase, after it was extracted from the circuit load line (such as R_L of Fig. 2), indicated a recombination time constant of 100ps.

Photoconductivity experiments were also conducted on Sample B having an increased ($3.93 \times 10^{15} cm^{-2}$) fluence relative to Sample A ($2.45 \times 10^{15} cm^{-2}$). One drawback of an increased fluence and, thus an increased density of recombination centers, is that the on-state conductivity is reduced because electrons in the conduction band 12 recombine with holes in the valence band 20 before those holes can be trapped in the Cu_B center. This interaction of the electrons and holes of the bands 12 and 20 reduces the number of holes that are trapped in the Cu_B center which, in turn, reduces the available sites to receive electrons from the valence band 20 during the turn-off laser pulse (laser beam 38 of Fig. 2(A)). However, a benefit can be derived if the density of recombination centers in the bulk material is made high enough to cause the BOSS switch 22 to open without the need of the turn-off laser beam 38. This effect is shown in Fig. 7 where two 1μm laser pulses, shown as waveforms 102 and 104 in Fig. 7 but respectively equivalent to laser beams 36 and 38 of Fig. 2(A), were used to close Sample B (that is, obtain its low resistance state) at a high repetition rate. For these experiments, the BOSS switch 22 was only illuminated by two 1μm laser pulses with a variable time delay between them shown in Fig. 7 by dimensional line 106. The reason

why Sample B opened without the turn-off laser pulse was because it was irradiated at a higher neutron fluence than Sample A. Therefore, there was a higher density of recombination centers in the bulk material of Sample B than that of Sample A. The purpose of this experiment with Sample B was twofold, first to see how the BOSS switch 22 (Sample B) responded to the turn-on laser pulse (laser beam 36 of Fig. 2(A)), and secondly, to test the repetition rate capability of Sample B. The applied voltage that created pulses 102 and 104 shown in Fig. 7 was about 16kV. The minimum on-state resistance that was measured for Sample B was about 15Ω. The average pulse width of both pulses 102 and 104 was measured to be about 340ps. Further, the average pulse width of a third pulse 108, shown in Fig. 7 as being spaced apart from pulse 104 by dimensional line 106A, was about 340ps. The time separation between the two laser pulses 102 and 104 or between 102 and 108, was varied from about 3.5ns, corresponding to a repetition rate of roughly 285MHz, down to less than 1ns, corresponding to a repetition rate of greater than 1GHz. These repetition rates are basically four to five orders of magnitude higher than used in the operation of any other type of high-power photoconductive switch known to us.

The maximum voltage that was switched with Sample B was 18kV, yielding an average electric field of 36kV/cm. Again, this bias voltage (18kV) was limited by the bias-voltage modulator of the test equipment, rather than a physical limitation of the BOSS

switch 22. It is important to note that there was no indication of Sample B collapsing into a filamentary-current mode of conduction, known in the art, at any point in the switching cycle. This non-collapse is significant since almost all previously reported photoconductive switch experiments exhibit a transition into filamentary conduction, or lock-on, at average electric fields of ≥10kV/cm. A previously reported transition into filamentary conduction is disclosed by F. J. Zutavern and G.M. Loubriel, in the technical article "High-Power Optically Activated Solid-State Switches," A. Rosen and F. Zutavern, Eds., Boston: Artech House, 1994, Chapter 11, and herein incorporated by reference. One of the most striking attributes of the current pulses 102, 104 and 108 is that the BOSS switch 22 (Sample B) completely opens without the need of the 2μm laser pulse that would serve as laser beam 38 previously discussed with reference to Fig. 2(A).

Since one of the potential applications of a BOSS switch 22 is in an impulse or ultra-wide-band (UWB) radar, we wanted to examine the Fourier spectra of the waveforms in Fig. 7. The results of performing a 4096-point fast fourier transformation (FFT) on the data in Fig. 7 are shown in Fig. 8. Fig. 8 illustrates two plots 110 and 112, with plot 112 having the wider spacing of its peaks. Fig. 8 shows significant frequency content up to about 3GHz which was the bandwidth limit of the SCD5000 digitizer 94 of Fig. 5. The result of adjusting the delay between the two pulses 110 and 112 (respectively serving as laser beams 36 and 38 of Fig. 2(A)) can be

seen as a change in the number, and location, of the nulls in the spectra. For example, by changing the time delay from 1ns to 3.4ns, the spectral peak of 1GHz is changed to a null. More particularly, and with reference to Fig. 8, if the time delay is changed from 1ns to 3.4ns, the peaks 110A and 112A at 1GHz for plots 110 and 112, respectively, move to locations (valleys) generally indicated by reference numbers 110B and 112B respectively. The capability to change the generated spectrum by simply changing the optical delay between laser pulses 110 and 112 (more particularly, laser beams 36 and 38 of Fig. 2(A)) could be very useful in UWB radar applications, particularly if certain frequency bands are to be avoided.

The stripline configuration of the PSO source 60 of Fig. 4 was also experimentally tested in the practice of this invention. As previously described, the PSO generator 60 has two separate BOSS switches 22A and 22B connected at the same point (common transmission line 70) on the stripline 82 so that there will not be any current reflections off of the opened BOSS switch 22A or 22B when the other BOSS switch 22B or 22A is closed. It should be noted that when one of the BOSS switches 22A or 22B of Fig. 4 is closed, the potential across the other BOSS switches 22B or 22A is doubled, assuming that both BOSS switches 22A and 22B are biased at equal values with opposite polarities 66 and 68. Therefore, the BOSS switches 22A and 22B in the PSO configuration 60 of Fig. 4 should be able to withstand voltages that are twice as high as the

charge voltage, carried by charged transmission lines 62 and 64, on the BOSS switches 22A and 22B. The severity of this problem is limited since each BOSS switch 22A or 22B is only closed for less than one or two nanoseconds.

During our experimental testing, the PSO source 60, shown in Fig. 4, was also biased with a 40ns voltage pulse generated by the Klystron circuit 92 of Fig. 5. However, the output of the Klystron circuit 92 had to be divided between the positive and negative striplines, that is, transmission lines 62 and 64 shown in Fig. 4. Therefore, the maximum voltage that could be applied to each BOSS switch 22, during our experimental testing, was about 10kV.

Experiments were performed with two Sample B devices embedded in the PSO generator 60 shown in Fig. 4. As previously discussed, the Sample B devices, now to be described as BOSS switches 22A and 22B of Fig. 4, were neutron irradiated at a relatively high fluence of $3.93 \times 10^{15} cm^{-2}$. These BOSS switches 22A and 22B were biased with a 40ns voltage pulse with a maximum amplitude of about 9.5kV. Since these BOSS switches 22A and 22B were self opening (as previously discussed for Samples B), only the 1μm wavelength was used for the PSO generator 60 demonstration.

A special optical delay line was set up which divided 1μm and 2μm laser pulses into two pulses, each with one half of the total energy transmitted by the laser source 86, previously mentioned

with reference to Fig. 5. This optical circuit depicted in Fig. 9 takes both the fundamental (1μm) and the wavelength-doubled (2μm) laser pulses out of the OPG 88, previously mentioned with reference to Fig. 5, and delivers them to the two BOSS switches 22A and 22B in the PSO generator 60 in such a way as to permit easy adjustment of the optical paths. For the arrangement shown in Fig. 9, the 1μm pulse is shown as wavelength $\lambda/2$ and the 2μm pulse is shown as wavelength λ. Dichroic mirrors 114, 116, 118 and 120, arranged as shown in Fig. 9, were used to separate the two wavelengths (λ and $\lambda/2$), and 50:50 beam splitters 122 and 124 were used to make a second set of laser pulses (λ and $\lambda/2$). The optical delay line was further fitted with mirrors 126, 128, 130 and 134 arranged as shown. Optical rails comprising elements 114, 116 .... 132 were further fitted with 180° turning prisms 136, 138, 140, 142, 144 and 146, having anti-reflection coatings thereon to minimize the optical losses, which allowed a laser-pulse separation (λ and $\lambda/2$) to be more easily adjusted. The optical rails depicted in Fig. 9 could be replaced by computer-controlled optical devices.

For the arrangement of Fig. 9, the first laser pulse 36, previously described with reference to Fig. 2(A), is shown as $\lambda/2$ and the second laser pulse 38, also previously described for Fig. 2(A), is shown as λ. The setup shown in Fig. 9 could be configured either to create a single switching event with a variable delay between the turn-on and turn-off laser pulses 36 and 38, or to create a two-pulse burst by repetitively switching a single BOSS

switch 22A or 22B. In the second case, a first BOSS switch, such as 22A could be switched at repetition rates as high as 1GHz within a two-pulse (36 and 38) burst. With this setup, the second BOSS switch, such as 22B can be closed at any time relative to the first BOSS switch 22A. This includes closing the second BOSS switch 22B before the first BOSS switch 22A is opened.

The time-domain waveforms for a time delay between the 1μm laser pulses (serving as laser beam 36) of about 500ps and about 2ns are shown in Fig. 10 respectively by waveforms 148 and 150, with waveform 148 being represented by the darker lines therebetween. The time delay of about 500ps resulted in the formation of a single RF cycle (indicated as 148), or monocycle, with a duration of a little over 1ns. There is a considerable amount of pulse sharpening of waveform 148 of the positive half-cycle thereof that occurs as a result of the second BOSS switch 22B closing prior to the complete recovery (obtaining its high resistance state) of the first BOSS switch 22A. This effect occurs because the opposite polarity of the charge voltage, that is, the voltage carried by charge transmission lines 62 and 64, results in a cancellation of the voltage that is actually delivered to the CVR, previously discussed with reference to Fig. 5. The advantage of this overlapping method of operating of the two separate BOSS switches 22A and 22B is that slightly higher frequencies, relative to the non-overlapping operation, can be obtained. However, the voltage cancellation also reduces both the peak amplitude of the

negative half-cycle, such as 148A, as well as the total energy contained in the positive half-cycle, such as generally indicated as 148B. The peak amplitude imbalance can be corrected by biasing the second BOSS switch 22B at a slightly higher negative voltage than the first BOSS switch 22A. When the laser time delay is increased to about 2ns, the actual response of the first BOSS switch 22A, represented by waveform 150, is measured, as shown in Fig. 10. In a manner similar to that of waveform 148, waveform 150 has a negative half-cycle 150A and a positive half-cycle 150B. For the case of waveform 150, the negative half-cycle 150A is roughly the mirror image of its positive half-cycle 150B. The remaining differences in the peak amplitudes are the result of the bias-voltage modulator of the test equipment of Fig. 9, rather than the operation of the BOSS switches 22A and 22B.

The ability to vary the time between the positive and negative half-cycles has a dramatic effect on the spectrum of the waveform. Several important characteristics of the Fourier spectra, obtained from the waveforms in Fig. 10, are illustrated in Fig. 11 for waveforms 152 and 154. First, unlike the spectra shown in Fig. 8, related to the laser pulse separation of 1ns and 3.4ns, the spectra in Fig. 11, related to the laser pulse separation of 500ps (waveform 152) and 2.0ns (waveform 154), contain a significantly reduced dc component. As mentioned earlier with reference to the PSO generator 60 of Figs. 3 and 4, a reduction in the dc component will greatly increase the ability to radiate the pulse, generated

by the operation of BOSS switches 22A and 22B, out of an antenna. Secondly, there is a drastic effect on the spectrum of the bipolar pulse when cross-over distortion is intentionally created. The spectrum associated with the undistorted monocycle represented by waveform 152 has a bandwidth of roughly 150%. In other words, dividing the FWHM of the spectrum, which is about 1.5GHz, by the center frequency of the spectrum, which is about 1GHz, yields a bandwidth of 1.5. Notice that it is difficult, it not impossible, to apply the same definition of spectral bandwidth to the case when there is a 2.0ns separation between the positive and negative half-cycles, as shown for the waveform 154 of Fig. 11.

As previously discussed with reference to Fig. 8, and as now illustrated in Fig. 11, varying the time delay between the positive and negative half-cycles of each waveform 152 or 154, changes the number and location of the nulls in the spectrum. Also, since the energy in the pulse should be conserved, increasing the number of nulls, by increasing the time delay between the half-cycles, results in a higher power-spectral density in the peaks of the spectrum. This is shown in Fig. 11, where the relative magnitude of the lower-frequency peaks of the distorted waveform 154 are more than a factor of two greater than the peak of the spectrum associated with the monocycle 152. Note that, after further analysis, a slight increase in the energy associated with the distorted waveform 154 is expected due to the lack of cancellation of part of the positive half-cycle. The dominant mechanism for the

increased lower frequency content is associated with a reduction of the fundamental frequency of the waveform. The fundamental frequency is basically a sinewave with its positive and negative peaks coincident with the positive and negative peaks of the distorted waveform 154. For example, in Fig. 11, the distorted waveform 154 has a 2ns separation between the positive and negative peaks. This separation would therefore result in a fundamental frequency of 250MHz, which corresponds to the first peak of waveform 154 in the spectrum, as shown in Fig. 11.

The high repetition rates of the PSO generator 60 were not fully tested by the practice of our invention because of the limitation of our test equipment. However, since the operation of the BOSS switch 22 was demonstrated at about 1GHz, in a burst mode, and since the operation of two BOSS switches 22A and 22B in a PSO generator 60, such as that of Figs. 3 and 4, has also been demonstrated, it is reasonable to examine the effect of generating a short burst of RF cycles of megahertz repetition rates. To accomplish this, a potential RF output from a PSO generator 60 was simulated by replicating data similar to that shown in Fig. 10 for a laser pulse separation of 500ps, and a time separation between RF cycles of 1ns. The result of this data manipulation is shown in Fig. 12 where four RF cycles, shown as waveforms 156, 158, 160 and 162 (each having positive and negative peaks), at a 100MHz repetition rate, are illustrated within a total time window set at 80ns. Fig. 12 is an illustration of the type of waveforms that are

actually expected to be generated by PSO generator 60.

The power spectra of a single monocycle, such as waveform 152 of Fig. 11, as well as the waveforms 156, 158, 160 and 162 shown in Fig. 12, corrected for a burst repetition rate of 1kHz, are illustrated in Figs. 13 and 14, respectively for waveforms 164 and waveform 166 (shown in a cluster manner). The method by which the power spectrum shown in both Figs. 13 and 14 was calculated was by first performing a fast fourier transform (FFT) on the time-domain waveforms of Figs. 13 and 14 of the corresponding voltage on a 50-Ω load, such as R_L of Fig. 3. The data was then padded, as known in the art, with zeros so that the total time window of 80ns (see Fig. 12) corresponded to a 12.5MHz burst repetition rate, as far as the FFT was concerned. The amplitude of the resulting frequency-domain data of Figs. 13 and 14 was determined in units of volts. To obtain the power spectrum in the 50Ω load, the amplitude was squared and subsequently divided by 50. The resulting spectral amplitude could now be expressed in units of watts, however, this amplitude also corresponds to the 12.5MHz repetition rate. To scale the data for a 1kHz repetition rate (such as that shown in Fig. 13), the data was multiplied by the square of the ratio of 1kHz over 12.5MHz, or by a factor of 6.4×10^{-9}.

The spectrum for the single monocycle, shown in Fig. 13 as waveform 164, has a maximum amplitude of about 1.5 watts. However, as a result of the 10ns spacing between the RF cycles as shown in

Fig. 14, the spectrum for the four-pulse burst, shown in Fig. 14 by cluster waveform 166, is further subdivided into peaks which occur every 100MHz. As a result of the increased number of nulls in the spectrum (generally shown by dark valleys indicated as 166B), the power spectrum at each one of the peaks is increased considerably. In fact, the peak power increased from 1.5 watts (Fig. 13) to about 24 watts (Fig. 14), or a factor of 16. There are basically two reasons for this increase in the power spectrum. First, since the power spectrum for both the monocycle (Fig. 13) and the four-pulse burst (Fig. 14) were calculated for a 1kHz repetition rate, the total energy in the four-pulse burst (Fig. 14) is a factor of four higher than the monocycle (Fig. 13). The other factor of four comes from the subdivision of the spectrum into discrete peaks at every 100MHz as generally indicated in Fig. 14. In a similar manner, if ten pulses were generated within a single burst, the peak of the power spectrum would be increased by a factor of 100. A higher number of cycles in the burst would also have the effect of reducing the width of each one of the 100MHz peaks.

The same type of results are obtained when using the waveform distorted by separating the positive and negative half cycles, as shown in Fig. 15, to fabricate the four-pulse 168, 170, 172 and 174 (each having positive and negative peaks) burst. Note that this distortion results in an additional increase in the peak of the power spectrum, at lower frequencies, as shown in Fig. 16, wherein the lower frequency burst, such as pulse 176, has a peak which is

greater than the higher frequency pulse, such as pulse 182. These results indicate that the time delay between the positive and negative half-cycles dictates the shape of the envelope of the spectrum, while the cycle repetition rate within the burst dictates the placement of the various spectral peaks. The type of waveforms shown in Figs. 12 and 15, with their associated spectra shown in Figs. 14 and 16, respectively, may have considerable advantages for use in UWB-radar and other high-power microwave (HPM) generation applications.

It should now be appreciated that the present invention provides a BOSS switch that is able to transient from its on (closed) to off (open) state in the subnanosecond regime as presented in Figs. 6 and 7. The ability to open, that is, obtain a high resistance state, in the subnanosecond regime is achieved by enhancing the recombination center density in the bulk material through fast-neutron irradiation.

An additional benefit of neutron irradiation ~~in~~ bulk photoconductive switches, such as BOSS switch 22, is that it allows the operation of these devices at voltage levels far greater than that possible in non-irradiated devices. The high level operation is primarily achieved by the enhanced speed of response of the neutron irradiated BOSS switch 22. Therefore, the neutron irradiation can be used as a means of preventing, or increasing the threshold voltage for, the development of a breakdown of the BOSS

switch which results in the formation of current filaments known in the art. Thus, the power-handling capability of the BOSS switch is increased.

It should be recognized that an additional benefit can be derived from irradiating GaAs:Si:Cu with neutrons if the neutron fluence is elevated to a level that is high enough to create a sufficient number of recombination centers such that the BOSS switch will open back up following the termination of the turn-on, or 1μm, laser pulse. This effect has been demonstrated in Fig. 7. Furthermore, it has been demonstrated that the ability to open a BOSS switch in the subnanosecond regime also allows the repetitive operation of the BOSS switch to be in the gigahertz regime, also shown in Fig. 7.

It has been demonstrated that neutron irradiation allows a BOSS switch to be manufactured that is suitable for implementing the pulse-switch-out (PSO) generator illustrated in Figs. 3 and 4. The PSO generator has the distinct advantage of being able to change the radiated frequency, in a very short time period, simply by varying the optical delays of the laser pulses used to control the switches. One example of a suitable optical circuit that permits real-time tunability of the PSO RF source is depicted in Fig. 9.

It should be further appreciated that the PSO configuration

depicted in Figs. 3 and 4 has the ability to control both the number and location, in frequency, of the nulls in either the radiated spectrum or the spectrum of the waveform delivered to a load through a transmission line. The PSO generator acting as a source also allows the amplitude of the spectral peaks to be adjusted by varying the optical path lengths taken by the various laser pulses that are used to turn-on and turn-off the BOSS switch of the present invention. The laser source used to control the PSO generator can have a significant effect on the radiated spectrum by controlling the number of cycles contained in the burst of RF energy. And, since the BOSS switch 22 of the present invention has virtually no jitter, the coherence of the radiated waveform is controlled by the laser system. If the laser pulses used to control the PSO generator, more particularly the BOSS switches of the PSO generator, are coherent in time, then the radiated RF waveform will also be coherent in time. The ability to control the spectrum in this manner as provided by the present invention may offer considerable advantages in many applications including, but not limited to, wide-band radar, ultra-wide-band (UWB) radar, high-resolution radar, coherent radar, ground-penetrating radar, foliage-penetrating radar, impulse radar, electronic counter measures (ECM), electronic counter-countermeasures (ECCM), electronic warfare (EW), spread-spectrum communications, and high-power microwave (HPM) generation.

Although neutron irradiation has been described for enhancing

the recombination centers of the BOSS switches, other methods could be used for recombination-center generation in GaAs:Si:Cu material. These methods include high-energy charged-particle irradiation, such as using electrons or ions. It may also be possible to grow the bulk GaAs material with a higher recombination-center density.

The PSO generator could also be implemented with photoconductive devices that are not based on GaAs:Si:Cu. Other materials could be used to implement the PSO generator, provided their electron-hole lifetime is short enough, including GaAs, InP, CdS, SiC, AlGaAs, HgTe, CdTe, ZnSe, Si, diamond (C) and GaN. The electrical pulse widths generated by these devices could possibly not be precisely controlled, as in the case of GaAs:Si:Cu, however, there could still be a considerable amount of frequency agility if devices manufactured from these materials were self-opening in the subnanosecond regime.

Numerous other variations and modifications of the present invention may be readily apparent to those skilled in the art in light of the above teachings. It is therefore to be understood that the invention may be practiced other than as specifically described herein.

ABSTRACT OF THE DISCLOSURE

A photoconductive switching device is disclosed that has an enhanced speed of response so that its closed (low) and open (high) resistive states are obtained in response to optical illumination in the less than nanosecond regime. The enhanced speed of response is achieved by neutron irradiation of a material preferably comprising GaAs:Si:Cu. An application of the improved photoconductive switching devices is disclosed which allows the realization of a high-power, frequency-agile RF source topology.

DOCKET. NAVY CASE 76,968
INVENTORS: D.C. Stoudt & M.A. RICHARDSON

10

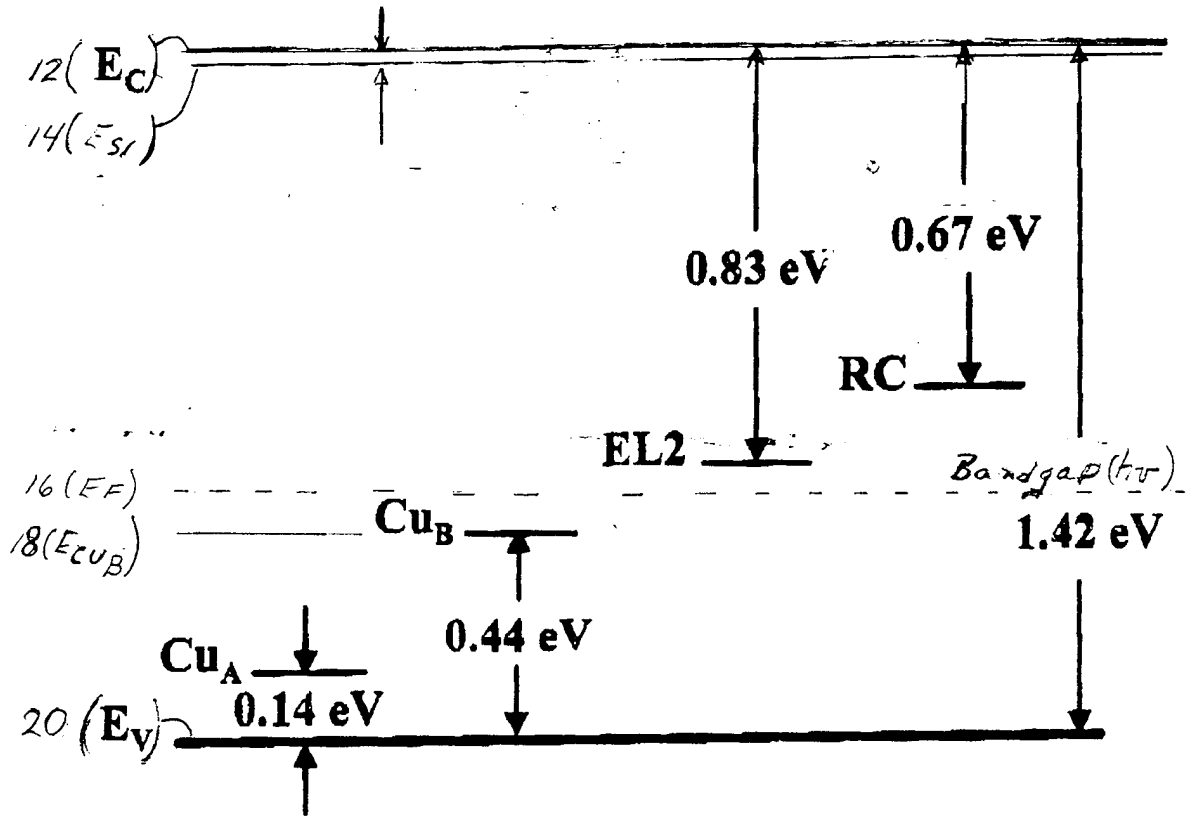

Fig. 1

DOCKET 10,760

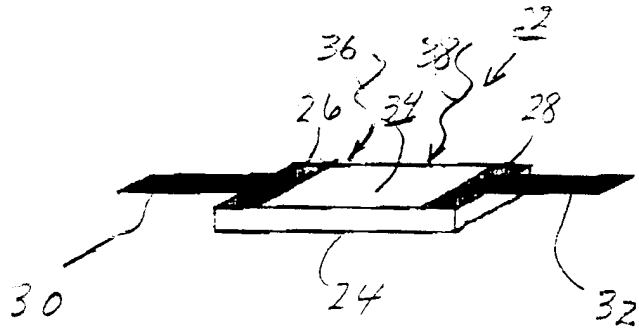

Fig 2 A)

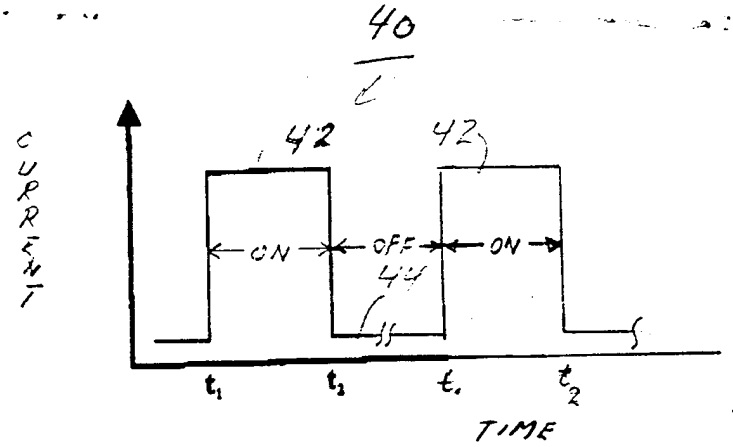

Fig 2 (B)

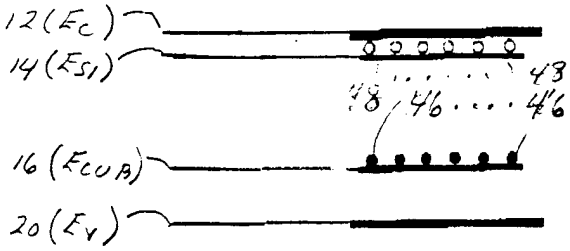

Fig 2 (C)

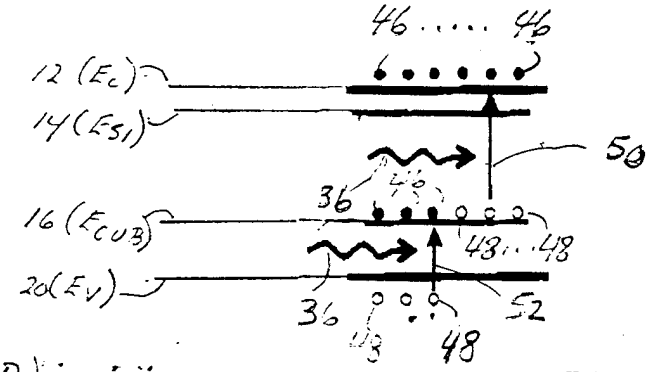

Fig 2 (D)

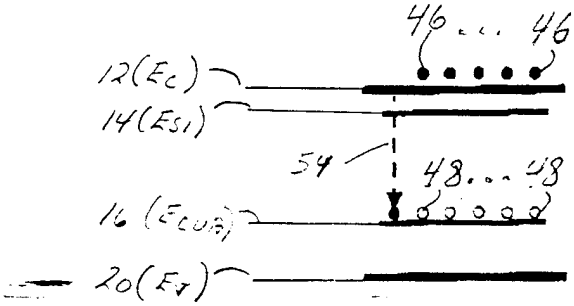

Fig 2 (E)

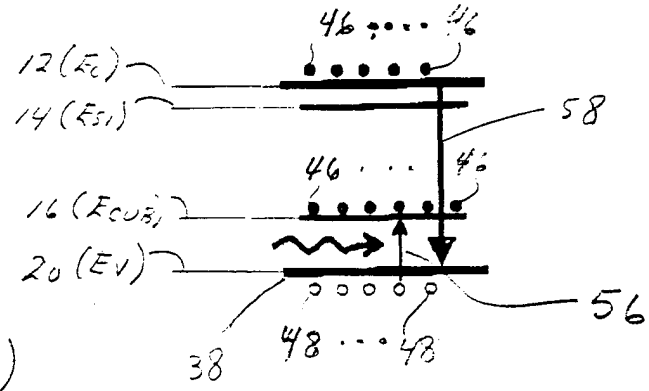

Fig 2 (F)

DOCKET 76,968

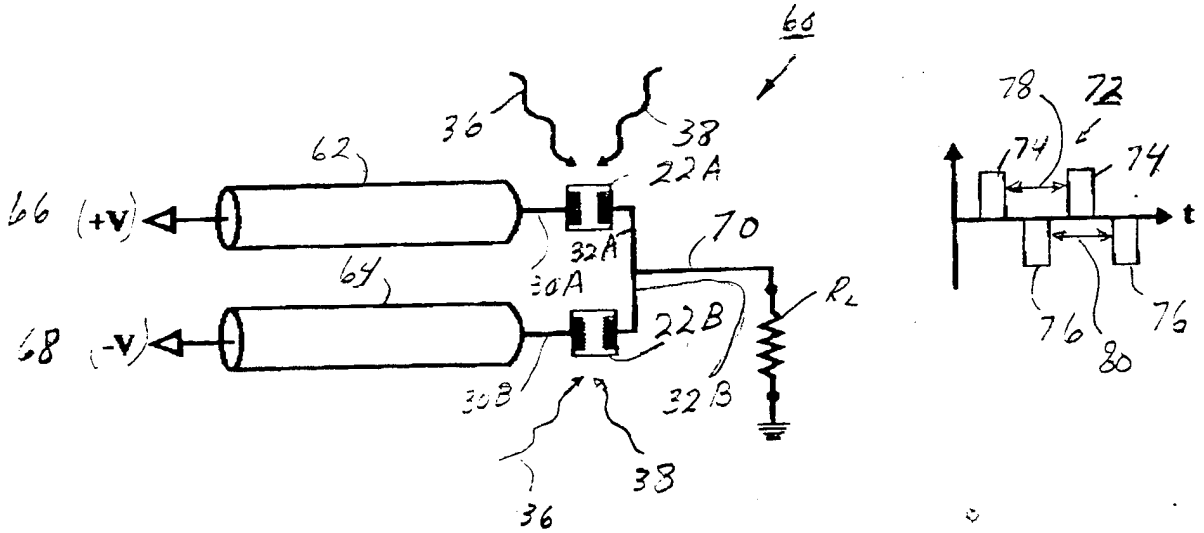

Fig. 3

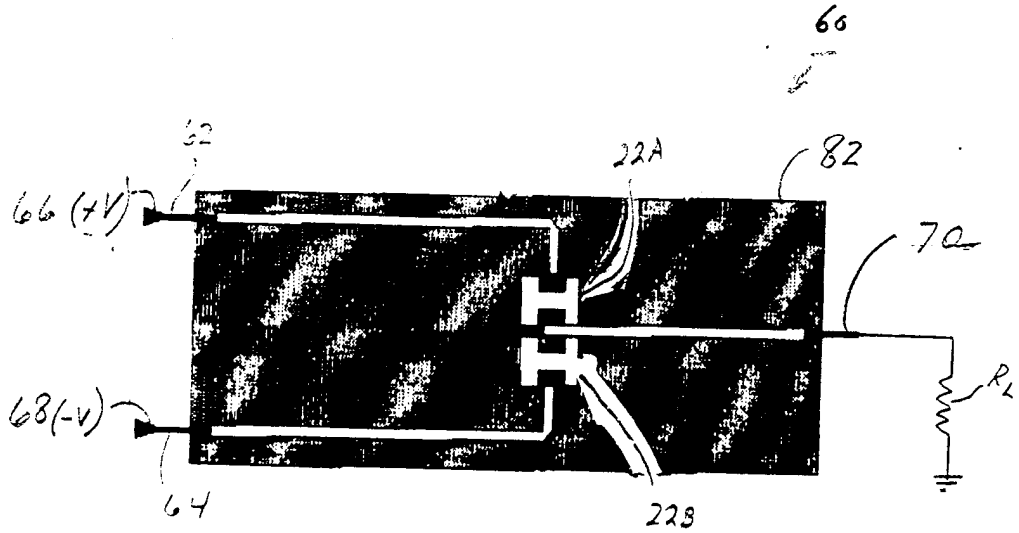

Fig 4

DOCKET 76,968

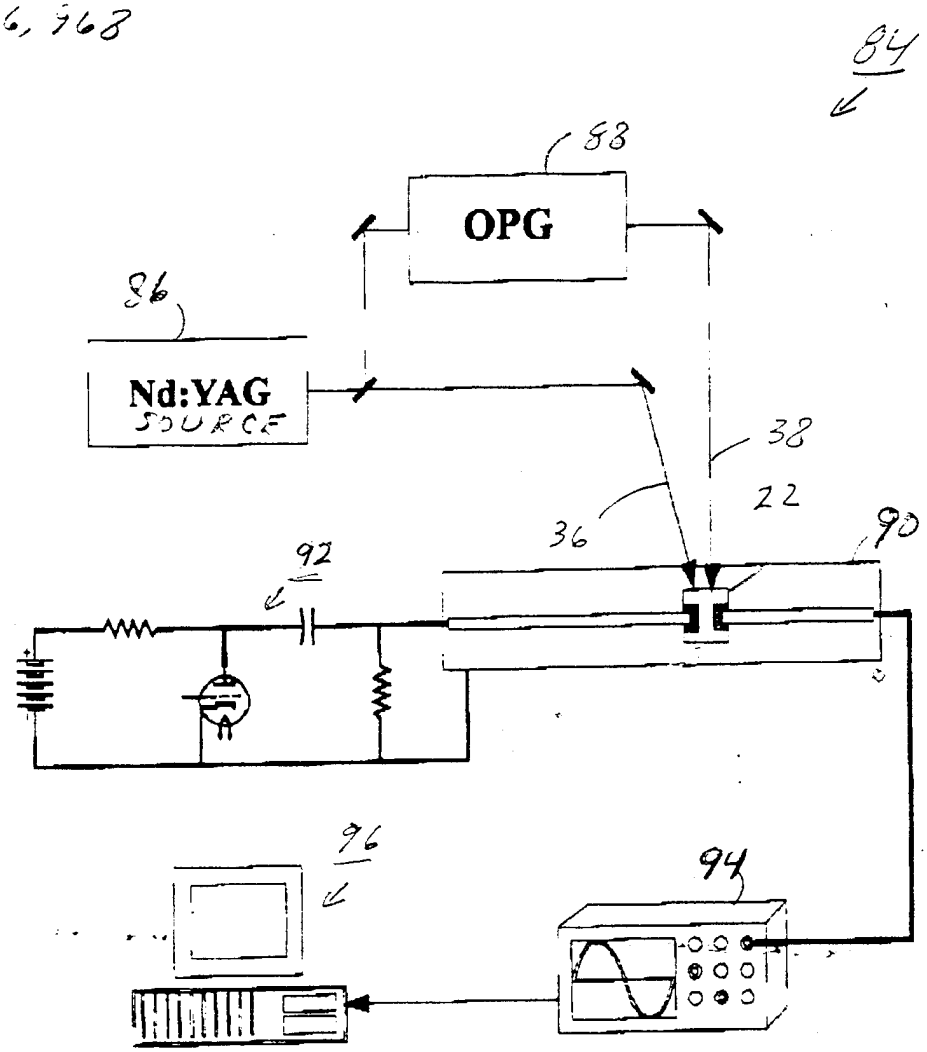

FIG. 5

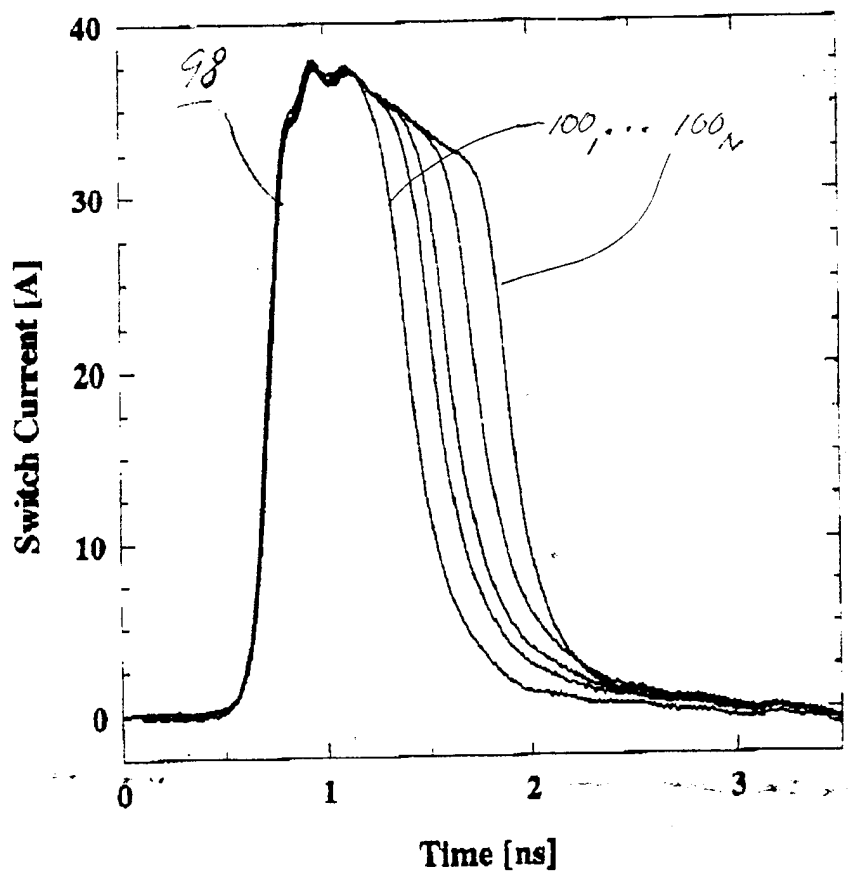
40
30
20
10
0
Switch Current [A]
0
1
2
3
Time [ns]
98
100₁ ... 100_N

Fig 6

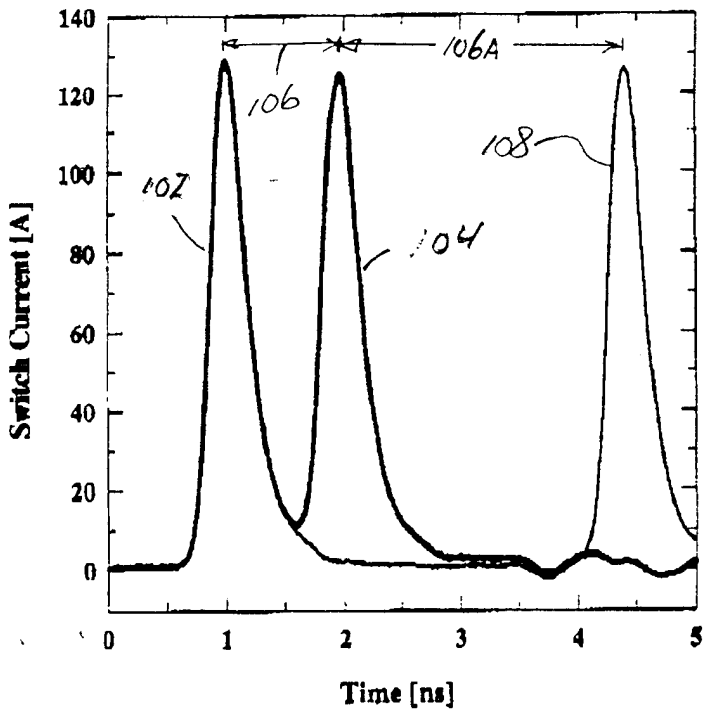
140
120
100
80
60
40
20
0
Switch Current [A]
0
1
2
3
4
5
Time [ns]
106A
106
108
102
104

Fig. 7

DOCKET 76,968

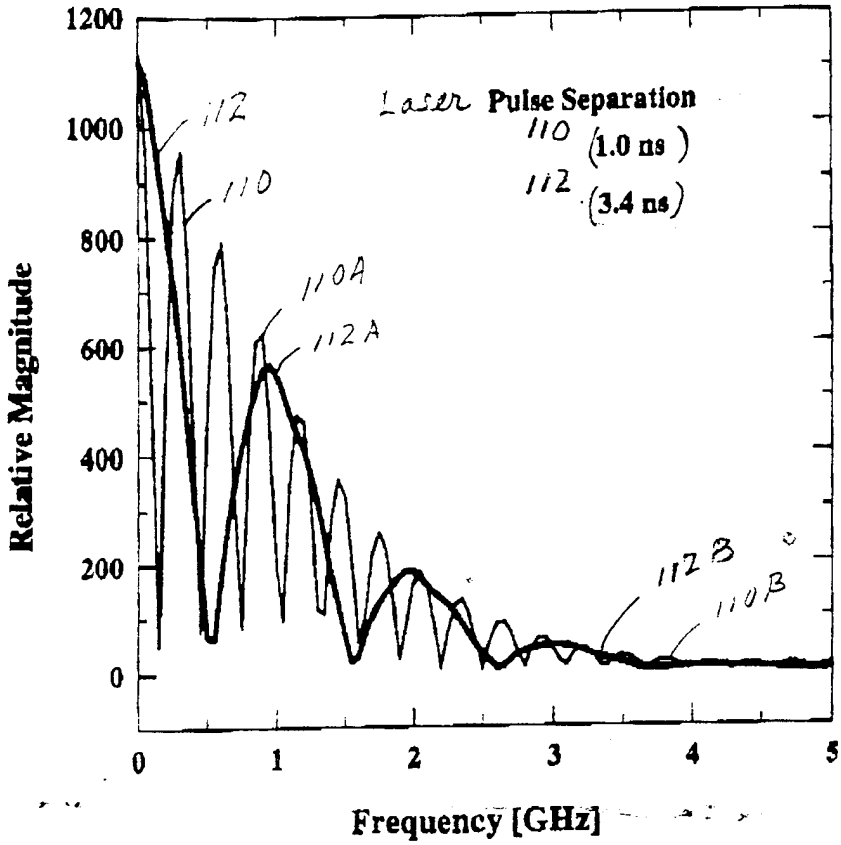

Fig. 8

DOCKET 76,968

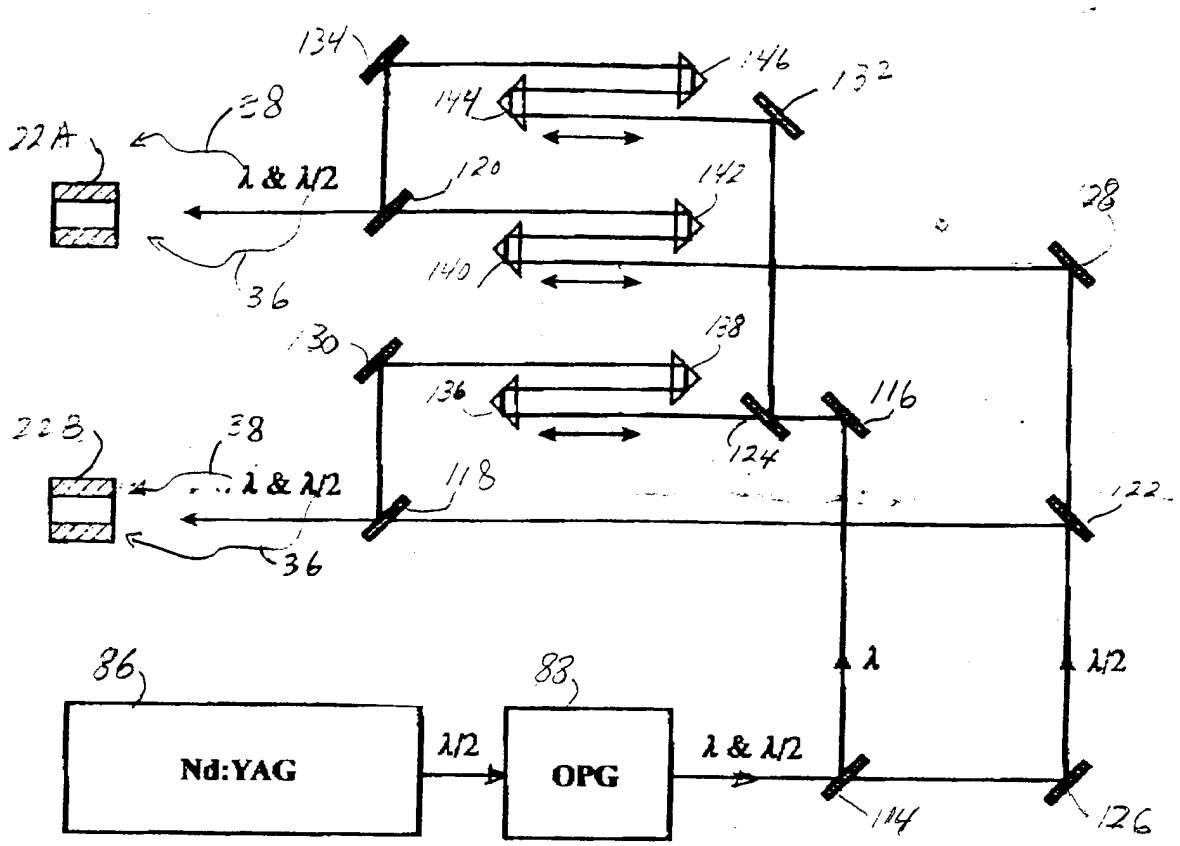

Fig 9

Docket 16,968

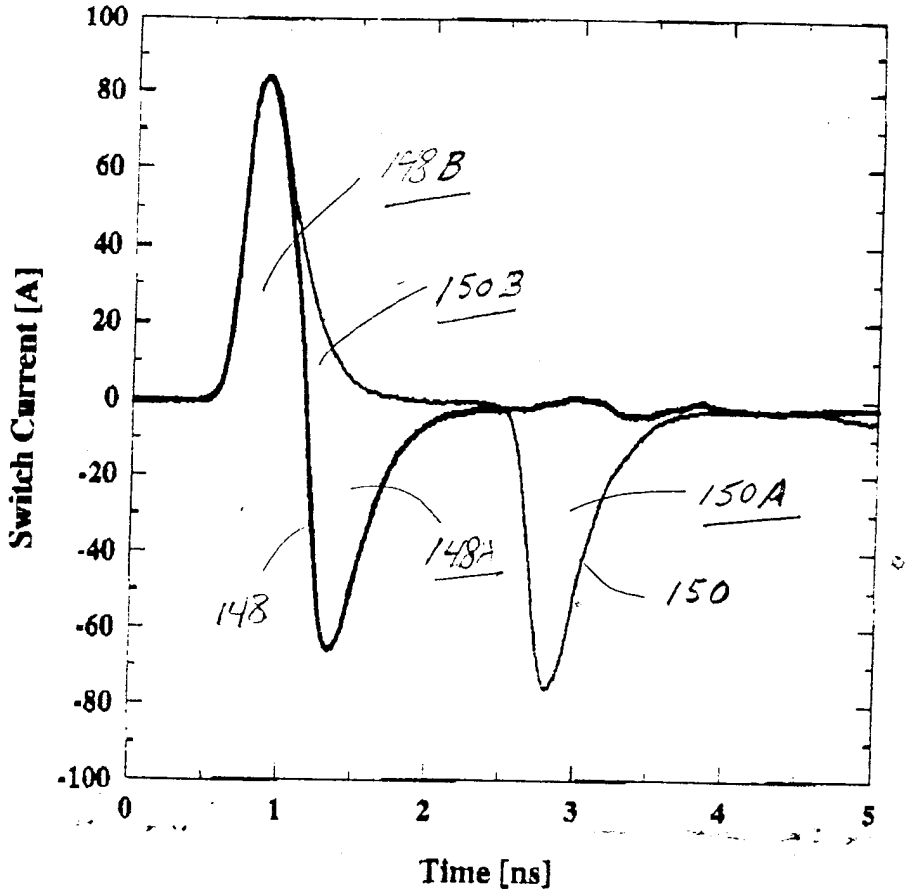

Fig. 10

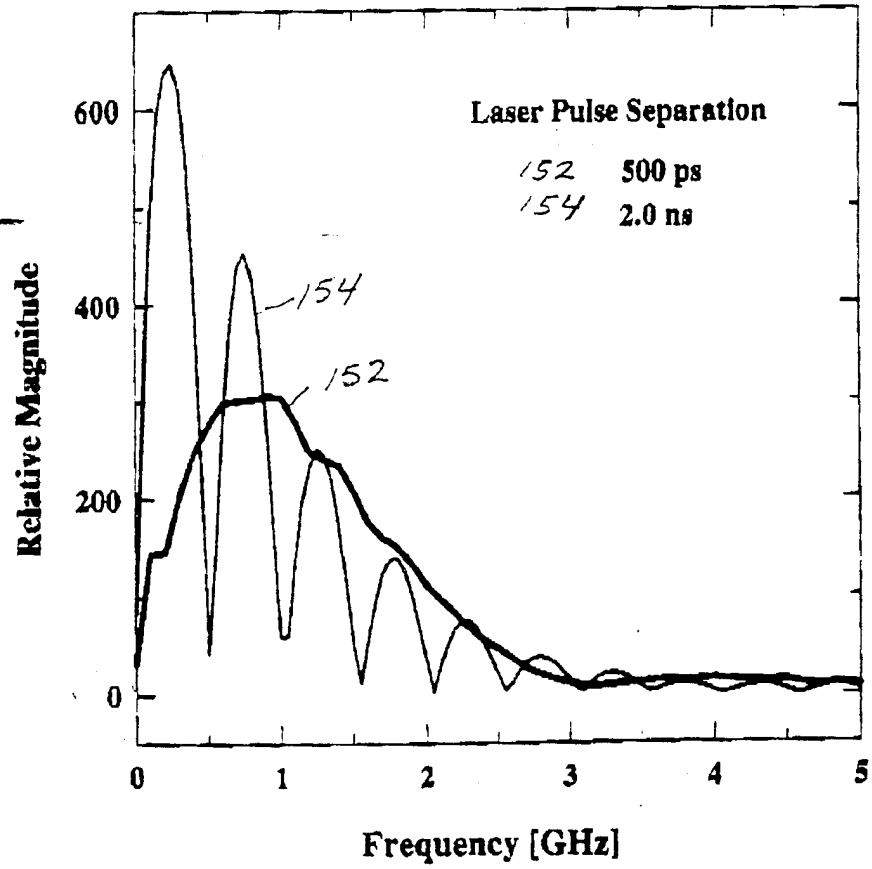

Fig 11

DOCKET 76,968

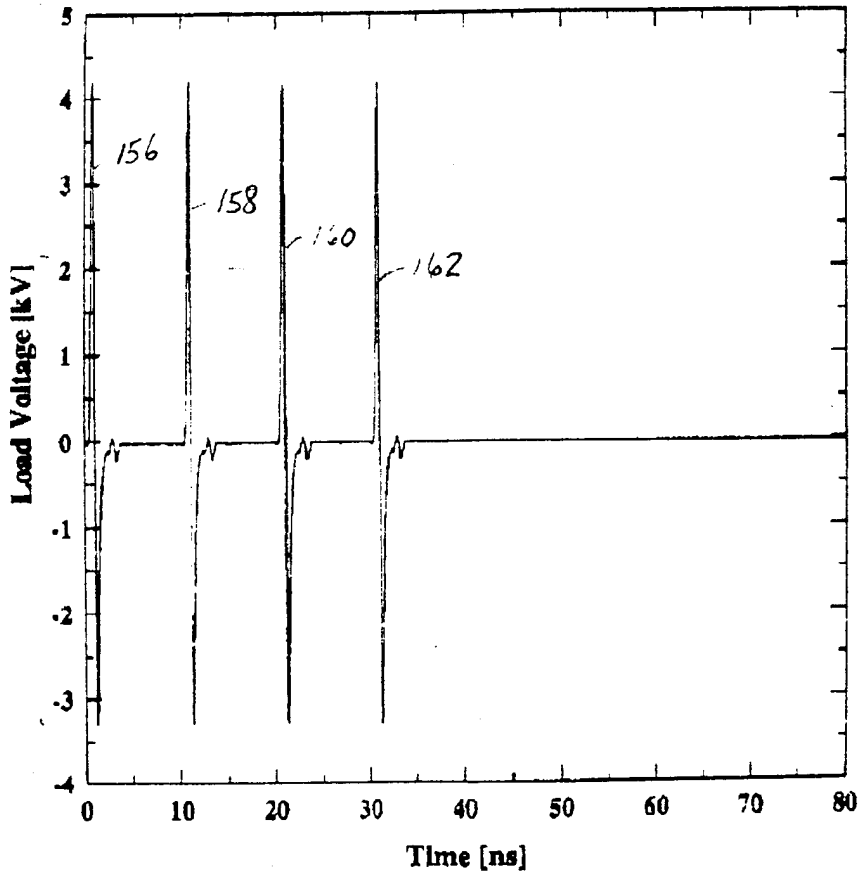

Fig. 12

DOCKET 76,968

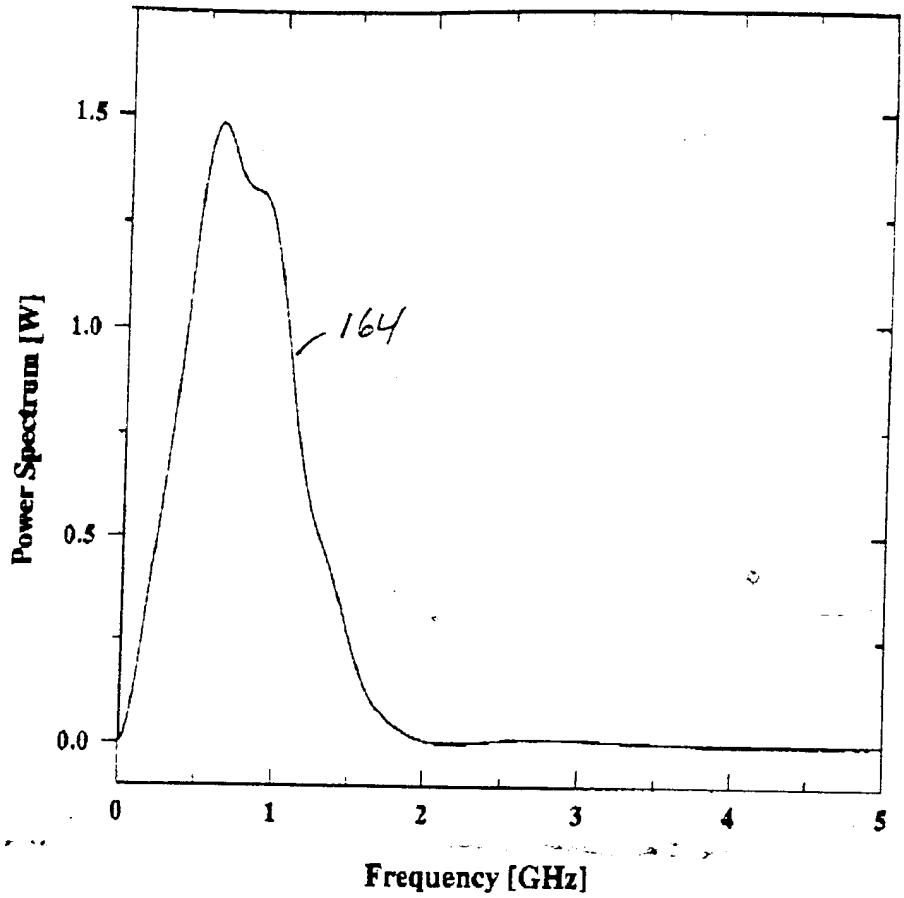

Fig. 13

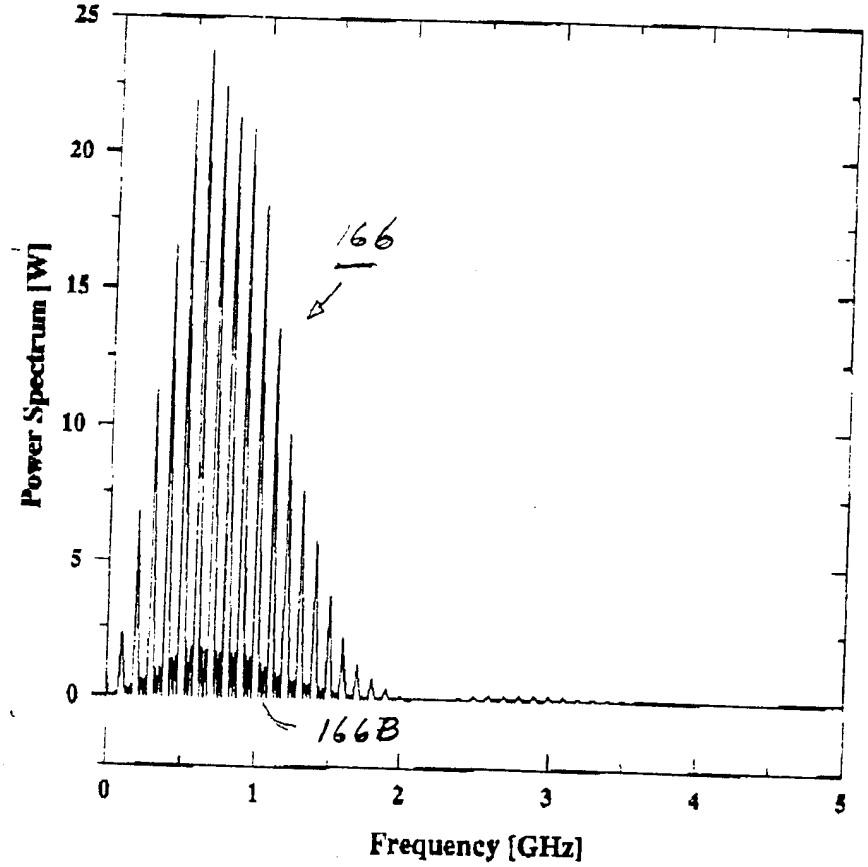

Fig. 14

DOCKET 76,968

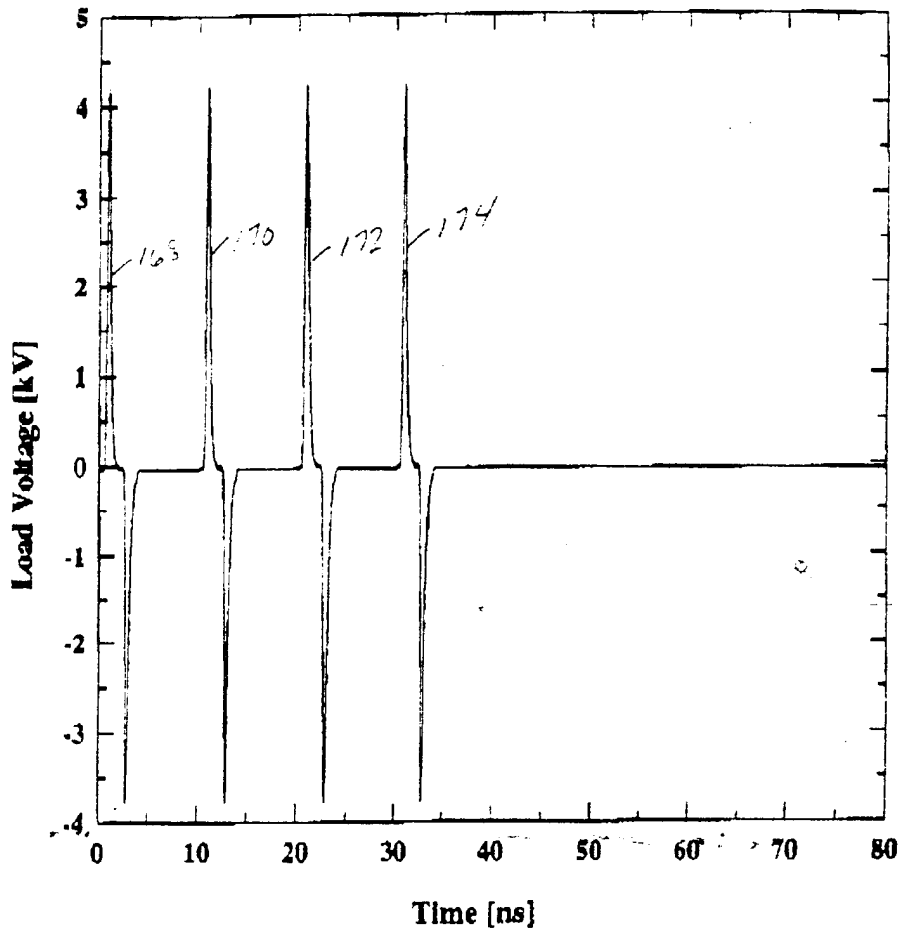

Fig. 15

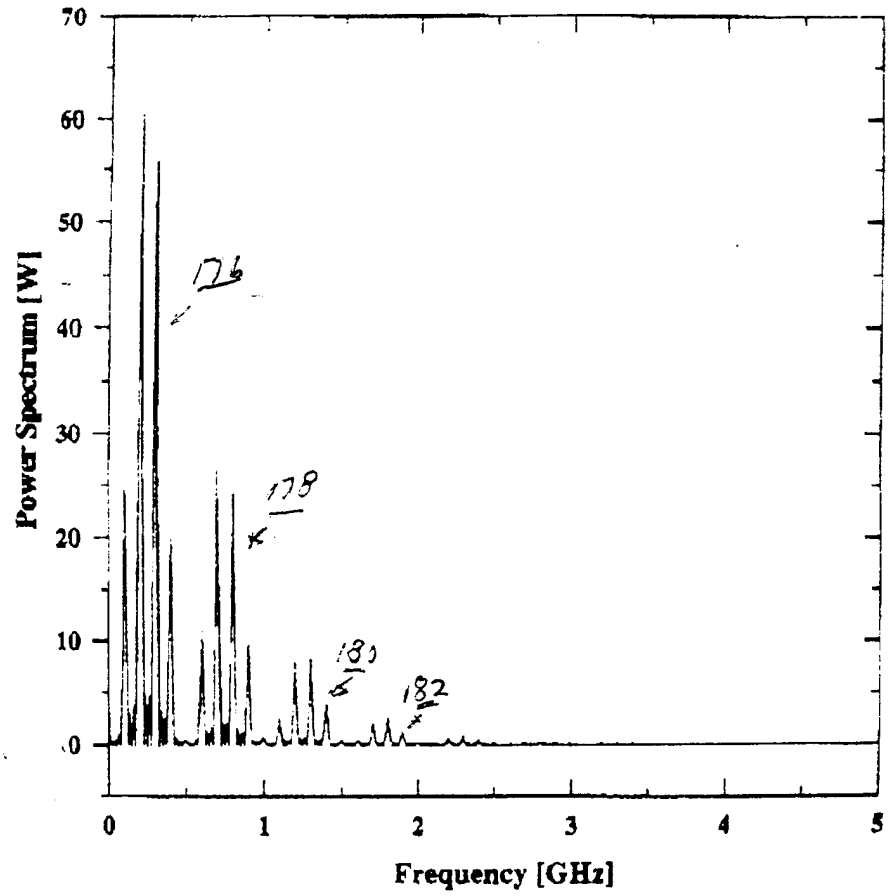

Fig. 16